

REPORT

Adherens junctions influence tight junction formation via changes in membrane lipid composition

Kenta Shigetomi¹, Yumiko Ono¹, Tetsuichiro Inai² , and Junichi Ikenouchi^{1,3} 

Tight junctions (TJs) are essential cell adhesion structures that act as a barrier to separate the internal milieu from the external environment in multicellular organisms. Although their major constituents have been identified, it is unknown how the formation of TJs is regulated. TJ formation depends on the preceding formation of adherens junctions (AJs) in epithelial cells; however, the underlying mechanism remains to be elucidated. In this study, loss of AJs in α -catenin-knockout (KO) EpH4 epithelial cells altered the lipid composition of the plasma membrane (PM) and led to endocytosis of claudins, a major component of TJs. Sphingomyelin with long-chain fatty acids and cholesterol were enriched in the TJ-containing PM fraction. Depletion of cholesterol abolished the formation of TJs. Conversely, addition of cholesterol restored TJ formation in α -catenin-KO cells. Collectively, we propose that AJs mediate the formation of TJs by increasing the level of cholesterol in the PM.

Introduction

Recent advances in lipidomics and lipid visualization tools revealed that membrane lipids are essential regulators of various membrane structures such as microvilli (Ikenouchi et al., 2013; Nicolson, 2014). Numerous membrane structures have characteristic morphologies such as tight junctions (TJs) in epithelial cells. TJs are cell adhesion structures that act as a barrier to prevent paracellular diffusion of solutes and water (Tsukita et al., 2001) and to stop infectious microorganisms entering the body. In pathological conditions such as inflammatory bowel diseases, asthma, and atopic dermatitis, the barrier function of TJs is impaired. Compromised epithelial barrier function underlies these chronic inflammatory diseases (Barmeyer et al., 2015; Tokumasu et al., 2016).

TJs are observed as a set of continuous, anastomosing strands in freeze-fracture EM; however, the molecular organization of TJ strands remains controversial (Pinto da Silva and Kachar, 1982; Lingaraju et al., 2015). Claudins, which have four transmembrane domains, are the major component of TJs and have been intensely studied (Zihni et al., 2016; Shigetomi and Ikenouchi, 2018). Nusrat et al. (2000) reported that claudins are present in detergent-resistant membranes (DRMs). However, the lipid composition of isolated membranes containing TJs has not been reported, and the roles of lipids in the function and formation of TJs remain unclear.

Although the molecular mechanisms underlying TJ formation are poorly understood, this process requires the preceding

formation of adherens junctions (AJs). TJs do not form when the formation of AJs is blocked (Gumbiner et al., 1988; Watabe-Uchida et al., 1998). Although the formation of AJs and TJs is closely related, the underlying mechanism is unclear (Hartsock and Nelson, 2008). It has long been assumed that AJs assist the formation of TJs by bringing the plasma membranes (PMs) of neighboring cells into close proximity; however, this assumption has not been directly tested.

In this study, we found that loss of AJs altered the subcellular distribution of cholesterol. The enrichment of cholesterol in the PM was decreased in α -catenin-knockout (KO) cells, and cholesterol was essential for the retention of claudins in the PM and the formation of TJs.

Results and discussion

Distribution of claudins in α -catenin-KO epithelial cells

To clarify the relationship between the formation of AJs and TJs, we knocked out α -catenin in cultured EpH4 epithelial cells using the CRISPR-Cas9 system (Fig. 1, A and B). In these cells, claudin-3 was present in cytoplasmic vesicles (Fig. 1 C). Other components of TJs such as occludin and JAM-A were also internalized in these cells, and the total level of claudin-3 was markedly reduced (Fig. 1 C). Exogenous expression of GFP- α -catenin restored the formation of AJs and TJs in these cells (Fig. 1, D and E).

¹Department of Biology, Faculty of Sciences, Kyushu University, Fukuoka, Japan; ²Department of Morphological Biology, Fukuoka Dental College, Fukuoka, Japan; ³Agency for Medical Research and Development-PRIME, Japan Agency for Medical Research and Development, Tokyo, Japan.

Correspondence to Junichi Ikenouchi: ikenouchi.junichi.033@m.kyushu-u.ac.jp.

© 2018 Shigetomi et al. This article is distributed under the terms of an Attribution-Noncommercial-Share Alike-No Mirror Sites license for the first six months after the publication date (see <http://www.rupress.org/terms/>). After six months it is available under a Creative Commons License (Attribution-Noncommercial-Share Alike 4.0 International license, as described at <https://creativecommons.org/licenses/by-nc-sa/4.0/>).

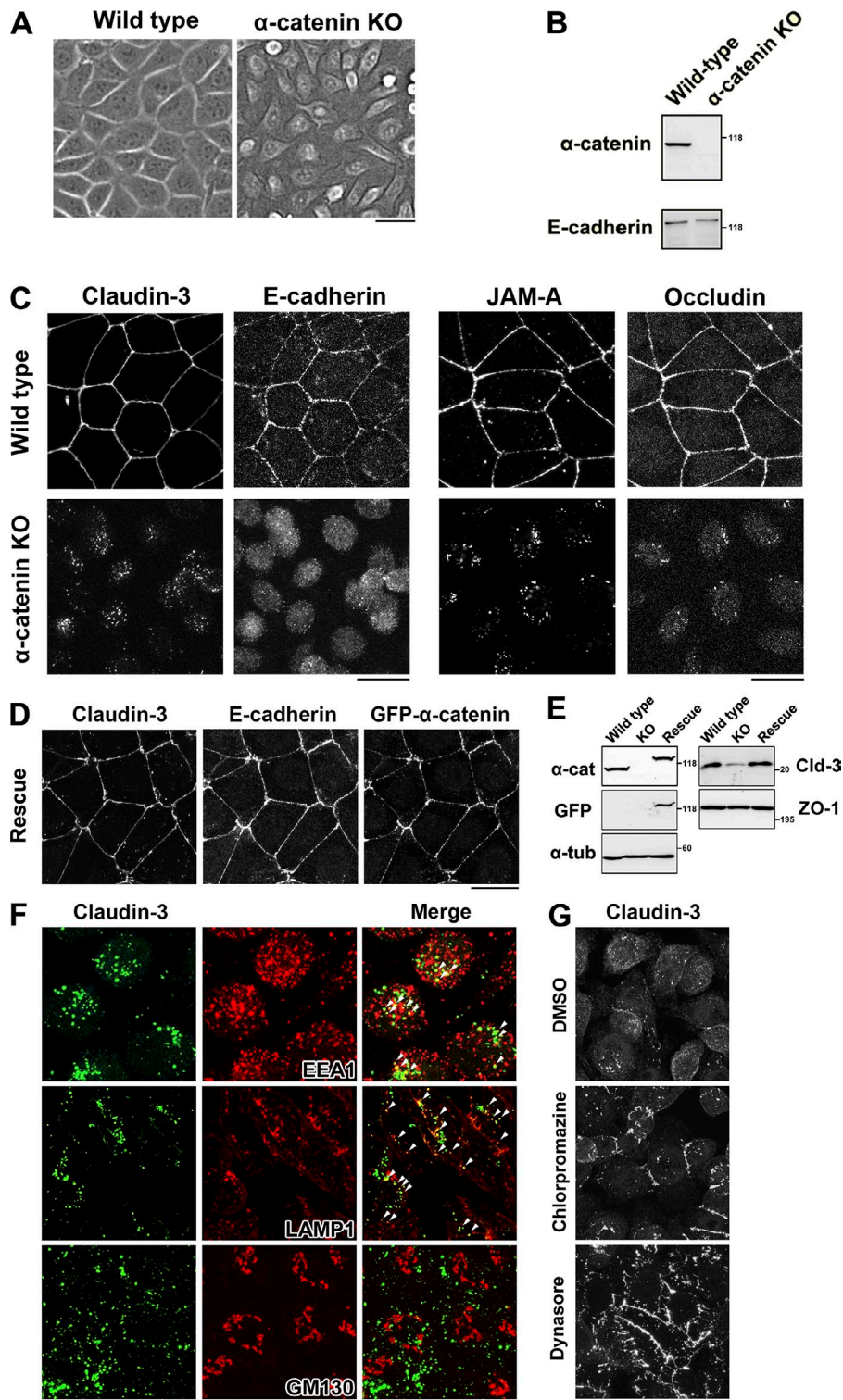


Figure 1. α -Catenin-KO cells internalize claudins. (A) Phase-contrast images of WT and α -catenin-KO Eph4 cells. (B) Immunoblotting of whole-cell lysates of WT and α -catenin-KO Eph4 cells with the indicated antibodies. (C) WT and α -catenin-KO Eph4 cells were fixed and costained with an anti-claudin-3 pAb and an anti-E-cadherin mAb (left) or with an anti-JAM-A pAb and an antioccludin mAb (right). (D) α -Catenin-KO Eph4 cells stably expressing GFP-tagged mouse α -catenin were fixed and costained with an anti-claudin-3 pAb and an anti-E-cadherin mAb. (E) Immunoblotting of whole-cell lysates of WT Eph4 cells, α -catenin-KO Eph4 cells, and α -catenin-KO Eph4 cells stably expressing GFP-tagged α -catenin (rescue) with the indicated antibodies. Molecular masses are given in kilodaltons. (F) α -Catenin-KO Eph4 cells were fixed and costained with an anti-claudin-3 pAb (green) and an anti-EEA1 mAb (red, top), an anti-LAMP1 mAb (red, middle), or an anti-GM130 mAb (red, bottom). Arrowheads indicate colocalization. (G) α -Catenin-KO Eph4 cells were treated with DMSO (control, top), 10 μ g/ml chlorpromazine (middle) for 1 h, or 100 μ M dynasore (bottom) for 2 h, fixed, and stained with an anti-claudin-3 pAb. Bars: (A, C, D, and F) 20 μ m; (G) 25 μ m.

Cytoplasmic vesicles containing claudin-3 were prominent in α -catenin-KO cells (Fig. 1 C). These vesicles partially colocalized with the early endosome marker EEA1 and the lysosome marker LAMP1 but not with the Golgi marker GM130, suggesting that claudins were endocytosed and degraded in lysosomes in these cells (Fig. 1 F). Treatment with inhibitors of endocytosis such as chlorpromazine and dynasore partially restored the retention of claudin-3 in the PM of α -catenin-KO cells (Fig. 1 G). These data

suggest that stable localization of claudins in the PM depends on the formation of AJs.

The subcellular distribution of cholesterol is altered in α -catenin-KO epithelial cells

The association of membrane proteins with lipid rafts was recently reported to affect their subcellular localizations (Diaz-Rohrer et al., 2014). To investigate why claudins were removed

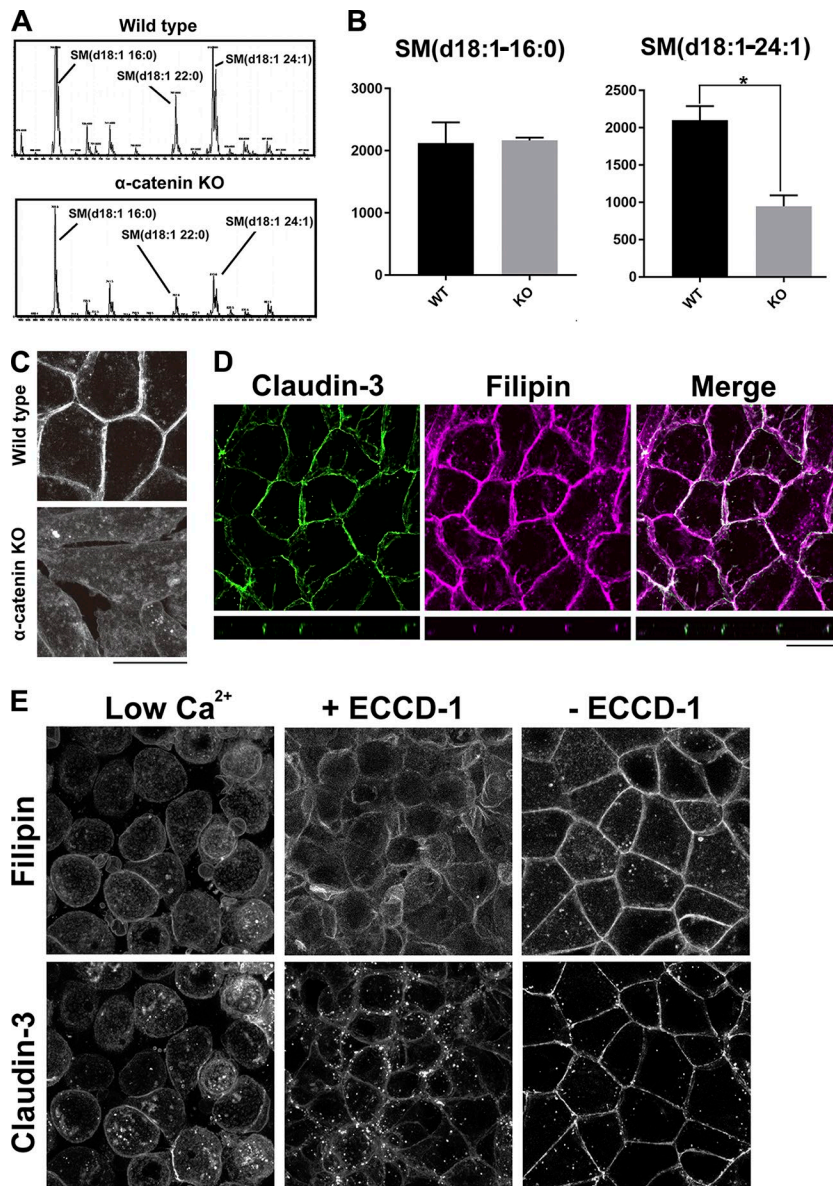


Figure 2. The level of cholesterol is reduced in the PM of α -catenin-KO cells. (A) Positive ion mass spectra of SM species in WT and α -catenin-KO EpH4 cells. The SM molecular species corresponding with each peak are indicated. The x and y axes show the total carbon chain length and the number of carbon-carbon double bonds of individual lipid molecular species, respectively. The results are representative of three independent experiments. (B) Quantification of the indicated SM species in WT EpH4 cells and α -catenin-KO EpH4 cells. Error bars show SD calculated based on three independent experiments (Student's *t* test, *, $P < 0.05$). (C) WT and α -catenin-KO EpH4 cells were fixed with 4% paraformaldehyde and stained with 50 μ g/ml filipin prepared in PBS to visualize the subcellular localization of cholesterol. (D) WT EpH4 cells expressing GFP-claudin-3 were fixed with 4% paraformaldehyde and stained with 50 μ g/ml filipin prepared in PBS. (E) Confluent WT EpH4 cells expressing GFP-claudin-3 were cultured in low-Ca²⁺ medium containing 5 μ M Ca²⁺ overnight to disrupt AJs completely (left) and then in normal Ca²⁺ medium containing ECCD-1 (1:500 dilution) for 1 h (middle). Thereafter, ECCD-1 was washed out, and cells were cultured in normal Ca²⁺ medium for 1 h (right). After fixation with 4% paraformaldehyde, cells were stained with 50 μ g/ml filipin prepared in PBS. Bars, 20 μ m.

from the PM in the absence of AJs, we compared the lipid profiles of WT and α -catenin-KO EpH4 cells. Total lipids were extracted from these cells according to the method of Bligh and Dyer. Lipid extracts were analyzed by electrospray ionization tandem mass spectrometry as previously reported (Ikenouchi et al., 2012). The profile of sphingomyelin (SM) species was altered in α -catenin-KO cells (Fig. 2 A). To analyze SM species, the positive ion mode spectra of these lipid extracts were compared. For peak assignment, each major ion was subjected to product ion scan analysis. There were three major molecular species of SM: SM (d18:1-16:0), SM (d18:1-22:0), and SM (d18:1-24:1) in WT cells. The level of very-long-chain SM (d18:1-24:1) was significantly lower in α -catenin-KO cells than in WT cells (Fig. 2 B).

SM species containing very long acyl chains preferentially interact with cholesterol and form membrane microdomains (Sezgin et al., 2017); therefore, we next examined the subcellular distribution of cholesterol using the cholesterol-binding

dye filipin. Enrichment of cholesterol in the PM was reduced in α -catenin-KO cells (Fig. 2 C). Of note, in WT cells, cholesterol was highly enriched at cell-cell contacts and partially colocalized with claudin-3 (Fig. 2 D).

α -Catenin is involved in various signal transduction pathways including the Hippo pathway (Takeichi, 2018). Consequently, the decrease in cholesterol in the PM of α -catenin-KO cells may occur independently of loss of AJs. Therefore, we investigated whether the distributions of cholesterol and claudins in the PM were affected when the formation of AJs was inhibited by an E-cadherin-blocking antibody (ECCD-1; Ogou et al., 1983).

We first treated confluent WT cells with low-Ca²⁺ medium containing 5 μ M Ca²⁺. The level of very long chain SM (d18:1-24:1) decreased as compared with the level of SM (d18:1-16:0), when AJs were gradually destroyed by the treatment with low-Ca²⁺ medium (Fig. S1 A). The enrichment of cholesterol in the PM was decreased by the treatment with low-Ca²⁺ medium for 6 h (Fig. S1 B).

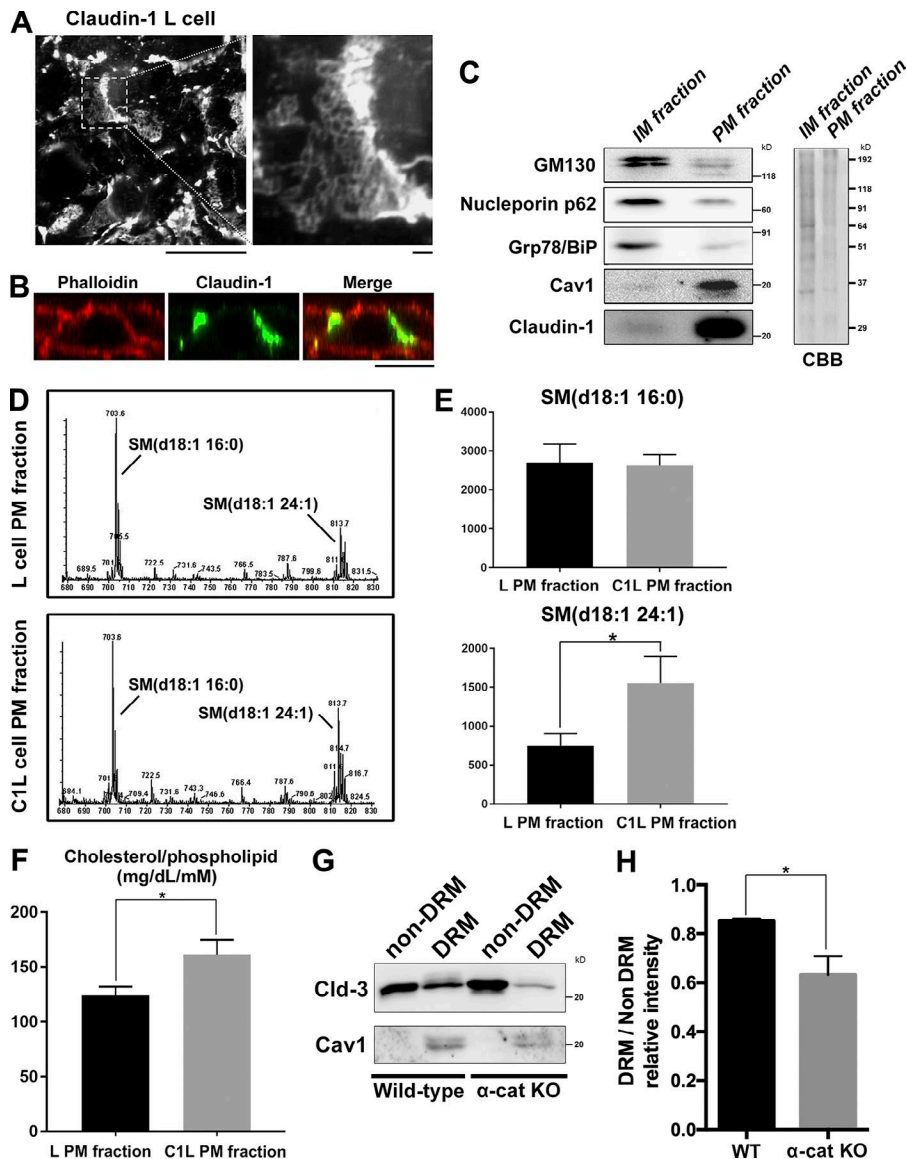


Figure 3. Cholesterol is enriched in the TJ-containing PM fraction. (A) C1L cells were fixed and stained with an anti-claudin-1 pAb. (B) C1L cells were fixed and stained with an anti-claudin-1 pAb (green) and phalloidin (red). Bars, 10 μ m. (C) Immunoblot analysis of the PM and IM fractions of C1L cells. Each membrane fraction (5 μ g) was separated by SDS-PAGE, transferred to a nitrocellulose membrane, and probed with antibodies against the indicated marker proteins (left). Coomassie brilliant blue (CBB) staining is shown on the right. (D) Positive ion mass spectra of SM species in the PM fractions of L and C1L cells. The SM molecular species corresponding with each peak are indicated. The x and y axes show the total carbon chain length and the number of carbon-carbon double bonds of individual lipid molecular species, respectively. (E) Quantification of the indicated SM species in the PM fractions of L cells and C1L cells. (F) Quantification of the cholesterol-to-phospholipid ratio in the PM fractions of L and C1L cells. (G) Immunoblot analysis of the DRM and non-DRM fractions of WT and α -catenin-KO EpH4 cells using pAbs against the DRM marker proteins claudin-3 and caveolin-1. Results in C, D, and G are representative of three independent experiments. (H) Quantification of the ratio of the claudin-3 level in the DRM fraction to that in the non-DRM fraction in WT and α -catenin-KO EpH4 cells. Error bars show SD calculated based on three independent experiments (Student's *t* test, *, *P* < 0.05).

Confluent WT cells were cultured in low- Ca^{2+} medium containing 5 μM Ca^{2+} overnight to disrupt AJs completely and then in normal Ca^{2+} medium containing ECCD-1. In both types of medium, claudin-3 remained in cytoplasmic vesicles, and cholesterol did not accumulate in the PM (Fig. 2 E). When ECCD-1 was washed out and AJs rapidly formed, the accumulation of cholesterol in the PM and the formation of TJs were restored (Fig. 2 E). Collectively, we conclude that loss of AJs impairs strong enrichment of cholesterol at the PM.

SM species containing very long acyl chains and cholesterol are enriched in the TJ-containing PM fraction

To examine whether reduction of cholesterol in the PM of α -catenin-KO cells perturbs the formation of TJs, we analyzed the lipid profile of the TJ-containing PM fraction. Detergents cannot be used to isolate this fraction because they accelerate mixing of lipids between different membrane fractions; therefore, it is technically difficult to obtain the TJ fraction of epithelial cells. Instead, we used claudin-1-expressing L (C1L) cells (Furuse

et al., 1998). L cells do not express any cell adhesion molecules. Whereas TJ formation requires the preceding formation of AJs in epithelial cells, exogenous expression of claudins is sufficient to induce TJ formation across the entire PM in L cells. In C1L cells, claudins formed huge networks of TJ strands across the entire cell surface at cell-cell contacts (Fig. 3 A).

We used the detergent-free colloidal silica method to isolate the PM fraction from these cells (Ikenouchi et al., 2012). In brief, cells were coated with cationic silica particles to increase the density of the PM membrane and then mechanically disrupted, and then the PM was obtained by gradient centrifugation. Claudin-1 was markedly enriched in the PM fraction (Fig. 3 B). However, levels of marker proteins of the inner-membrane (IM) fraction such as the Golgi marker GM130, the nuclear membrane marker NP62, and the ER marker Grp78/BiP were much lower in the PM fraction than in the IM fraction (Fig. 3 C). Next, we compared the lipid profiles of the PM fractions of parental L cells and C1L cells. The level of very-long-chain SM (d18:1-24:1) was significantly increased in the PM fraction of C1L cells as

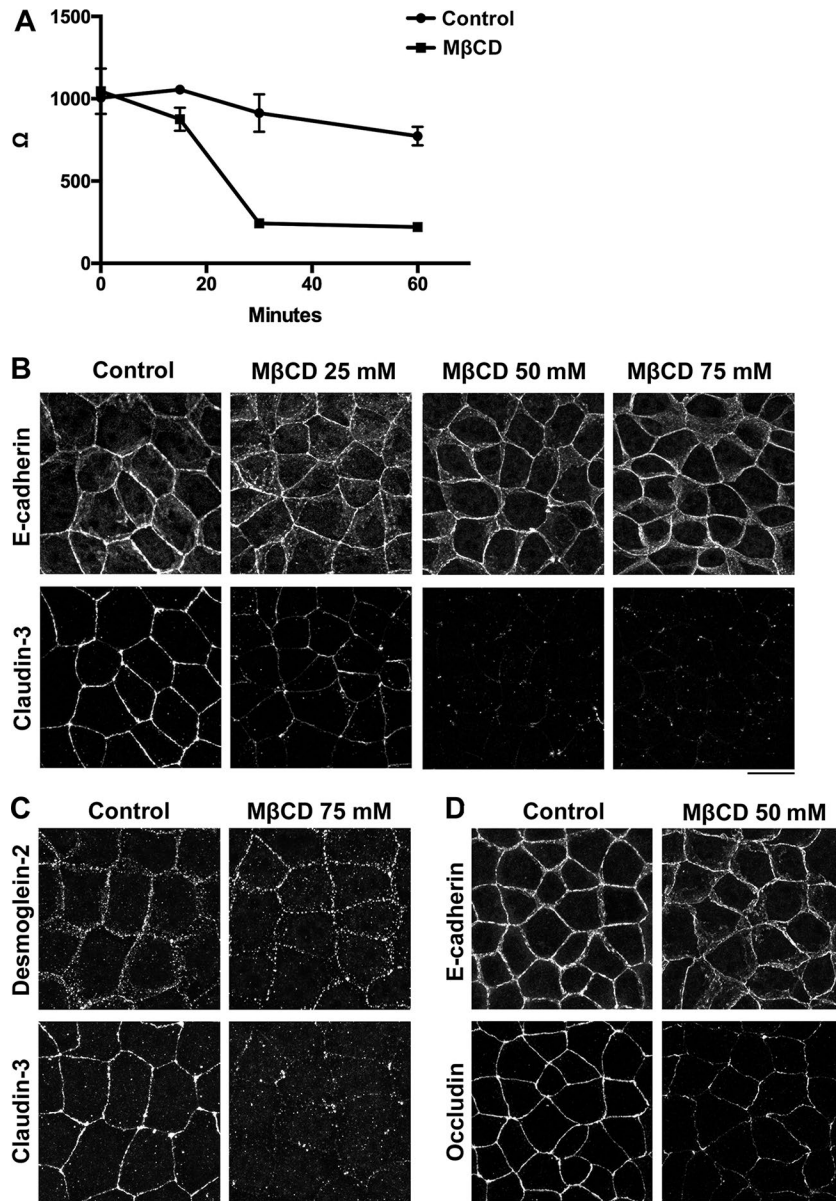


Figure 4. Depletion of cholesterol specifically impairs the formation of TJs. (A) WT EpH4 cells were cultured in transwell chambers and treated with PBS (control) or 75 mM MβCD for the indicated duration, and then cells underwent TER analysis (means ± SD; *n* = 4). (B) WT EpH4 cells were treated with PBS (control), 25 mM MβCD, 50 mM MβCD, or 75 mM MβCD for 30 min, fixed, and costained with an anti-claudin-3 pAb and an anti-E-cadherin mAb. (C) WT EpH4 cells were treated with PBS (control) or 75 mM MβCD for 30 min, fixed, and costained with an anti-claudin-3 pAb and an anti-desmoglein-2 mAb. (D) WT EpH4 cells were treated with PBS (control) or 50 mM MβCD for 30 min, fixed, and costained with an anti-E-cadherin mAb and an antioccludin pAb. Bars, 20 μm.

compared with the level of SM (d18:1-16:0; Fig. 3, D and E). In addition, the cholesterol level was significantly higher in the PM fraction of C1L cells than in that of parental L cells (Fig. 3 F). Collectively, we conclude that SM with very-long-chain fatty acids and cholesterol are enriched in the TJ-containing PM fraction. These findings suggest that claudins are preferentially found in the DRM fraction, in which SM species with very-long-chain fatty acids and cholesterol are enriched.

Therefore, we next examined whether the proportion of claudins in the DRM fraction differs between WT and α-catenin-KO cells. DRM fractions were directly purified using a Triton X-100 lysis method followed by separation via a sucrose gradient as previously reported (Nusrat et al., 2000). The proportion of claudin-3 in the DRM fraction was significantly reduced in α-catenin-KO cells (Fig. 3, G and H).

We next investigated whether depletion of cholesterol impairs the formation of TJs in epithelial cells. As previously reported (Francis et al., 1999), removal of cholesterol from the

PM via treatment with methyl-β cyclodextrin (MβCD) rapidly disrupted the barrier function of epithelial cells as revealed by measuring trans-epithelial resistance (TER; Fig. 4 A). Treatment with MβCD led to loss of claudins from cell-cell contacts in a dose-dependent manner but did not affect the localization of E-cadherin or desmoglein-2 (Fig. 4, B and C). As previously reported (Francis et al., 1999), occludin was more resistant to cholesterol depletion than claudins because staining of occludin was only attenuated upon treatment with ≥50 mM concentrations of MβCD (Fig. 4 D). These results indicate that claudins are more sensitive to a reduction in cholesterol than other cell adhesion molecules in epithelial cells.

Addition of cholesterol restores the formation of TJ strands in α-catenin-KO cells

Our results indicate that TJs form when cholesterol is enriched at the PM. However, concentration of cholesterol at the PM was decreased in α-catenin-KO cells. Therefore, we hypothesized that

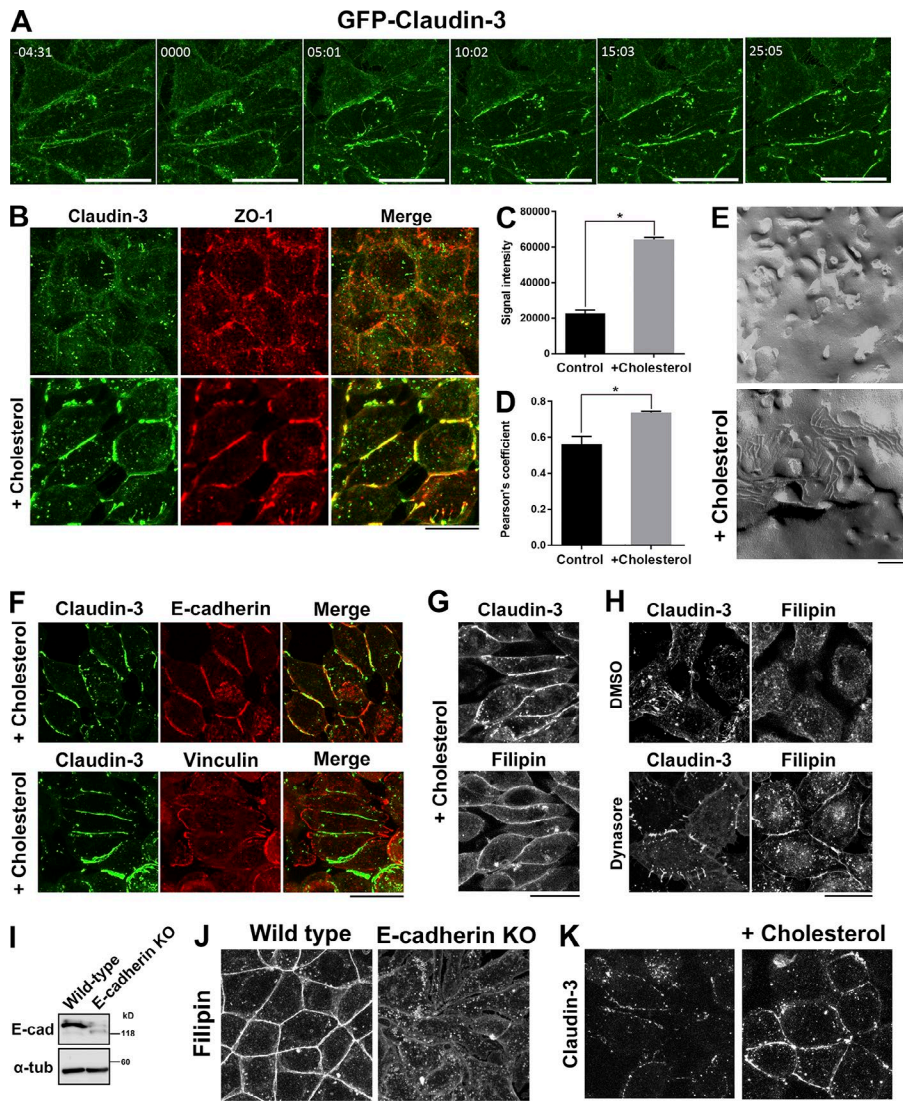


Figure 5. Addition of cholesterol to the PM induces TJ strand formation in α -catenin-KO cells. (A) Time-lapse imaging of α -catenin-KO EpH4 cells expressing GFP-claudin-3. At time 0, 75 mM cholesterol-saturated M β CD was added to the medium to restore the level of cholesterol in the PM. (B) α -Catenin-KO EpH4 cells were treated with PBS (control) or 75 mM cholesterol-saturated M β CD, fixed, and costained with an anti-claudin-3 pAb (green) and an anti-ZO-1 mAb (red). (C) Quantification of the signal intensity of claudin-3 at cell-cell contact areas in α -catenin-KO EpH4 cells before and after loading of cholesterol in the PM. (D) Quantification of the colocalization of claudin-3 and ZO-1 in α -catenin-KO EpH4 cells before and after loading of cholesterol in the PM. The degree of colocalization between claudin-3 and ZO-1 was calculated using ImageJ Fiji software. The value of Pearson's coefficient of two signals were quantitated. Error bars show SD calculated based on four independent experiments (Student's *t* test, *, *P* < 0.05). (E) Freeze-fracture EM images of TJ strands in α -catenin-KO EpH4 cells treated with PBS (control, top) or 75 mM cholesterol-saturated M β CD (bottom) for 30 min. (F) α -Catenin-KO EpH4 cells were treated 75 mM cholesterol-saturated M β CD, fixed, and stained with an anti-claudin-3 pAb (green) together with an anti-E-cadherin mAb (red, top) or an antivinculin mAb (red, bottom). (G) α -Catenin-KO EpH4 cells expressing GFP-claudin-3 were treated with 75 mM cholesterol-saturated M β CD, fixed with 4% paraformaldehyde, and stained with 50 μ g/ml filipin prepared in PBS. (H) α -Catenin-KO EpH4 cells expressing GFP-claudin-3 were treated with DMSO (control, top) or 100 μ M dynasore (bottom), fixed with 4% paraformaldehyde, and stained with 50 μ g/ml filipin prepared in PBS. (I) Immunoblotting of whole-cell lysates of WT and E-cadherin-KO EpH4 cells with the indicated antibodies. (J) WT and E-cadherin-KO EpH4 cells were fixed with 4% paraformaldehyde and stained with 50 μ g/ml filipin prepared in PBS. (K) E-cadherin-KO EpH4 cells were treated with PBS (control) or 75 mM cholesterol-saturated M β CD, fixed, and stained with an anti-claudin-3 pAb. Bars: (A, B, F-H, J, and K) 20 μ m; (E) 200 nm.

AJs mediate the formation of TJs by increasing the amounts of cholesterol in the PM.

Given that the level of cholesterol at the PM was reduced in α -catenin-KO cells, we investigated whether addition of cholesterol to the PM induces TJ strand formation in these cells. To this end, we treated α -catenin-KO cells with cholesterol-saturated M β CD. After this treatment, claudin-3 rapidly accumulated in the PM and concentrated at cell-cell contacts within 30 min (Fig. 5, A and B; and Video 1). We quantitatively measured the increase of signal intensity of claudin-3 at cell-cell contact areas in α -catenin-KO EpH4 cells after loading of cholesterol in the PM (Fig. 5 C). We also quantitatively measured the degree of colocalization between claudin-3 and ZO-1 in α -catenin-KO cells before and after addition of cholesterol. Addition of cholesterol increased the colocalization of claudin-3 and ZO-1 in

α -catenin-KO cells (Fig. 5 D). We also confirmed that TJ strands formed at cell-cell contacts by freeze-fracture EM (Fig. 5 E). The TJ strands that formed after addition of cholesterol were fragmented and nonfunctional because they did not circumferentially surround cells. Thus, the formation of AJs lined by the circumferential actin belt is essential for the formation of functional TJs. However, addition of cholesterol was sufficient to restore the formation of TJ strands even in the absence of AJs.

In addition to claudin-3, E-cadherin also accumulated at cell-cell contacts in α -catenin-KO cells treated with cholesterol-saturated M β CD (Fig. 5 F). However, E-cadherin is not bound to the actin cortex and is not under tension in α -catenin-KO because vinculin is absent from cell-cell contacts in α -catenin-KO cells (Fig. 5 F; Maddugoda et al., 2007). In α -catenin-KO cells treated with cholesterol-saturated M β CD, cholesterol accumulated at

the PM and colocalized with claudin-3 (Fig. 5 G). Treatment with dynasore partially restored the accumulation of cholesterol in the PM of α -catenin-KO cells, indicating that retention of claudins in the PM upon treatment with an endocytosis inhibitor is mediated by an increase in cholesterol in the PM (Fig. 5 H).

Next, to examine whether this restoration of E-cadherin in the PM is involved in the induction of TJ strands, we generated E-cadherin-KO EpH4 cells (Fig. 5 I). These cells were round and could not adhere with each other, similar to α -catenin-KO cells. The enrichment of cholesterol in the PM was reduced in E-cadherin-KO cells (Fig. 5 J). Upon treatment with cholesterol-saturated M β CD, TJ strands formed in E-cadherin-KO cells as observed in α -catenin-KO cells (Fig. 5 K). Therefore, we conclude that TJ formation is dependent on the presence of cholesterol, but not of E-cadherin, in the PM. Based on these findings, we propose that the lack of TJs in α -catenin-KO cells is primarily caused by the reduced level of cholesterol in the PM.

Concluding remarks

The expression pattern of lipid-metabolizing enzymes was thought to regulate the lipid composition of cells. However, our study demonstrates that the amount of cholesterol is changed in the PM of epithelial cells lacking AJs, although the underlying mechanism remains unclear. The insolubility of E-cadherin increases in the early stage of cell-cell contact formation in epithelial cells (McNeill et al., 1993; Hinck et al., 1994). During cell-cell contact formation, the actin cortex lining the cell membrane is reorganized (Acharya et al., 2017). On the other hand, the actin cortex promotes the formation of cholesterol-rich membrane domains (Chichili and Rodgers, 2009). Thus, cadherin-based cell adhesion may remodel the PM. It will be interesting to examine how accumulation of cholesterol at the PM occurs during cell-cell contact formation in a future study.

Similarly to cell-cell adhesion, cell-ECM adhesion markedly changes the composition of the PM. Adhesion of cells to the ECM via integrins facilitates the transport of cholesterol-enriched vesicles to the PM (del Pozo et al., 2004; Norambuena and Schwartz, 2011). This study showed that the amount of cholesterol in the PM was decreased when the formation of AJs was impaired. This suggests that cell-cell adhesion via AJs controls vesicular transport of cholesterol to the PM in addition to cell-ECM adhesion. Cholesterol is transported to the PM via a complicated pathway involving synthesis of cholesterol at the ER, nonvesicular transport of cholesterol from the ER to the TGN, and vesicular transport of cholesterol from the TGN to the PM (Mesmin and Antonny, 2016). Although our understanding of how integrin-mediated adhesion regulates vesicular transport of cholesterol is limited, it was recently reported that Arf6 and microtubules are involved in this process (Balasubramanian et al., 2007). In the case of cell-cell adhesion, AJs are crucial for the regular organization of microtubules in epithelial cells (Meng and Takeichi, 2009). Furthermore, Arf6 is activated at cell-cell contacts of epithelial cells (Ikenouchi and Umeda, 2010). It is important to clarify the molecular mechanisms by which the formation of AJs facilitates the transport of cholesterol to the PM in the future.

Materials and methods

Reagents

EpH4 cells and L fibroblasts were grown in DMEM supplemented with 10% FCS. α -Catenin-KO and E-cadherin-KO EpH4 cells were established using the CRISPR-Cas9 system. Oligonucleotides were phosphorylated, annealed, and cloned into the BsmBI site of the pLenti-CRISPR v2 vector according to protocols of the Zhang laboratory (Massachusetts Institute of Technology, Cambridge, MA). The target sequences for mouse α -catenin and mouse E-cadherin were 5'-CAATGATGAAAACGCCAAG-3' and 5'-ATTAGACGGCCCTTACTAT-3', respectively. Three independent clones were established for each construct.

The following primary antibodies were used for immunofluorescence microscopy and immunoblotting: rabbit anti-claudin-1 (71-7800), rabbit antioccludin (71-1500), rabbit anti-claudin-3 (34-1700), and rabbit anti-JAM-A (36-1700) polyclonal antibodies (pAbs; Thermo Fisher Scientific); mouse anti- α -tubulin mAbs and a rabbit anti- α -catenin pAb (Sigma-Aldrich); mouse anti-GM130, mouse anti-LAMP1, mouse anti-BiP/Grp78, and mouse antinucleoporin p62 mAbs (BD); a mouse anti-desmoglein-2 mAb (Abcam); a rabbit anti-caveolin-1 pAb (Cell Signaling Technology); a rabbit anti-syntaxin-3 pAb (Synaptic Systems); and mouse anti-ZO-1 (T8754), rat antioccludin (MOC37), and rat ECCD-2 mAbs (Takara Bio Inc.). Ascites fluid containing ECCD-1 was a gift from M. Takeichi (Center for Developmental Biology, Kobe, Japan). Chlorpromazine hydrochloride, cholesterol, dynasore hydrate, and M β CD were purchased from Sigma-Aldrich.

Fluorescence microscopy

Immunofluorescence microscopy was performed as described previously (Shiomi et al., 2015). In brief, cells cultured on coverslips were fixed with 3% formalin prepared in PBS for 10 min at RT, treated with 0.4% Triton X-100 prepared in PBS for 5 min, and washed with PBS. Fixed cells were blocked with 5% BSA prepared in PBS for 30 min at RT. Antibodies were diluted in this blocking solution. Cells were incubated with primary antibodies for 1 h at RT and with secondary antibodies for 30 min at RT. Specimens were observed at RT with a confocal microscope (LSM700; ZEISS) equipped with a Plan Aplanachromat objective (63 \times 1.40 NA oil-immersion objective) with appropriate binning of pixels and exposure times. Images were analyzed with ZEN 2012 (ZEISS). To visualize the subcellular localization of cholesterol, cells were fixed with 4% paraformaldehyde and stained with 50 μ g/ml filipin (Sigma-Aldrich) prepared in PBS.

Live-cell imaging

Fluorescence imaging was performed using a 63 \times oil-immersion objective on an inverted microscope (LSM700; ZEISS) interfaced with a laser-scanning confocal microscope equipped with a stage heated to 37°C as described previously (Aoki et al., 2016). Images were captured on a device camera and acquired on a personal computer using ZEN 2012 software (LSM700; ZEISS). Images were acquired using an excitation wavelength of 488 nm. Each frame is an eight-bit grayscale image, and the frame interval is indicated in the legend.

Freeze-fracture EM

Freeze-fracture EM was performed as described previously (Shiomi et al., 2015). Confluent cells were fixed with 2.5% glutaraldehyde prepared in phosphate buffer, rinsed with phosphate buffer, mixed with 30% glycerol prepared in phosphate buffer, and frozen in liquid propane. Frozen samples were fractured at -110°C and underwent unidirectional platinum shadowing at an angle of 45° in a JFD-7000 apparatus (JEOL). Replica samples were immersed in household bleach to remove cells and were mounted on copper grids. Samples were examined using a JEOL 2000EX electron microscope.

Isolation of the PM using colloidal silica

The PM fraction was isolated from L and CIL cells using the method of Stolz et al. (1992) with slight modifications. In brief, L and CIL cells were washed twice with coating buffer (CB; 135 mM NaCl, 20 mM MES, 1 mM Mg^{2+} , and 0.5 mM Ca^{2+} , pH 5.5) and coated with 1% (wt/vol) cationic colloidal silica prepared in CB. Thereafter, cells were washed with CB, coated with 1 mg/ml polyacrylic acid prepared in CB, pH 5.0, and washed again with CB. Shear force was applied to the cells by squirting them with CB containing a protease inhibitor cocktail using a 5-ml syringe fitted with a flattened 18-gauge needle (Nacalai Tesque). Samples were observed underneath a light microscope to confirm that all cells had been lysed. The lysate was mixed with the same amount of 100% (wt/vol) Nycodenz prepared in CB and sedimented through a cushion of 85% (wt/vol) Nycodenz prepared in CB. Dense silica-coated PMs were pelleted by centrifugation at 100,000 g (PM fraction). The supernatant was also retained as the IM fraction.

Lipid analysis

Lipids extracted using the Bligh and Dyer method were subjected to electrospray ionization tandem mass spectrometric analysis as previously described (Ikenouchi et al., 2012). In brief, cultured cells (10^6) were washed with PBS three times, and lipids were extracted by Bligh and Dyer's method. Concentrated lipid extract was dissolved in 100 μl of chloroform/methanol (2:1). The electrospray ionization mass spectrometry analysis was performed on a 6420 triple-quadrupole liquid chromatography-mass spectrometer (Agilent Technologies) equipped with an HPLC system and an auto sampler (Infinity 1260; Agilent Technologies). The extracted phospholipids were directly subjected to electrospray ionization mass spectrometry analysis. The mobile phase composition was acetonitrile/methanol/water = 18:11:1 (0.1% ammonium formate). The flow rate was 4 $\mu\text{l}/\text{min}$. The mass range of the instrument was set at 650–950 m/z . Cholesterol was quantitatively measured using a total cholesterol assay kit (Cell Biolabs, Inc.) in accordance with the manufacturer's instructions.

TER measurement

Aliquots of 5×10^4 cells were plated on trans-well polycarbonate filter supports with a pore size of 0.4 μm and a diameter of 12 mm (Costar). The culture medium was changed every day. TER was measured directly in culture media using an epithelial voltohmmeter (Millicell-ERS; EMD Millipore) and corrected for fluid resistance between the potential-sensing electrodes.

Preparation of the DRM fraction

Confluent cells were washed with HBSS and incubated with 1% Triton X-100 prepared in HBSS for 30 min at 4°C . The DRM were isolated after flotation on a sucrose gradient as described previously (Nusrat et al., 2000).

Preparation of M β CD-cholesterol inclusion complexes

M β CD-cholesterol inclusion complexes were generated by mixing a cholesterol suspension with an M β CD solution. In brief, M β CD was dissolved in PBS to a concentration of 375 mM, and then cholesterol was added to a concentration of 0.1 g/ml. This saturated M β CD-cholesterol solution was incubated in a water bath at 37°C overnight. Immediately before use, the solution was filtered through a 0.22- μm syringe filter (EMD Millipore) to remove excess cholesterol crystals. This solution was added to the medium at a final concentration of 75 mM.

Online supplemental material

Fig. S1 shows changes of PM composition induced by treatment with low- Ca^{2+} medium. Video 1 shows time-lapse imaging of α -catenin-KO Eph4 cells expressing GFP-claudin-3.

Acknowledgments

We thank all members of the Ikenouchi laboratory (Department of Biology, Faculty of Sciences, Kyushu University, Fukuoka, Japan) for helpful discussions. We thank Akira Kubo for help at the initial phase of this study.

This work was supported by Japan Society for the Promotion of Science KAKENHI (JP16H04786 [J. Ikenouchi], JP16H01362 [J. Ikenouchi], JP17H06012 [J. Ikenouchi], JP16K14729 [J. Ikenouchi], JP15KT0152 [J. Ikenouchi], and JP17J00211 [K. Shigetomi]), Japan Agency for Medical Research and Development-PRIME (15664862), The Japan Science and Technology Corporation-Precursory Research for Embryonic Science and Technology (JPM JPR12A4), grants from the MSD Life Science Foundation and Takeda Science Foundation, and a Japan Society for the Promotion of Science Research Fellowship for Young Scientists (DC1; K. Shigetomi).

The authors declare no competing financial interests.

Author contributions: K. Shigetomi performed most of the experiments and analyzed the data. Y. Ono and T. Inai performed some of the experiments. J. Ikenouchi designed the research and wrote the paper.

Submitted: 8 November 2017

Revised: 23 March 2018

Accepted: 25 April 2018

References

- Acharya, B.R., S.K. Wu, Z.Z. Lieu, R.G. Parton, S.W. Grill, A.D. Bershadsky, G.A. Gomez, and A.S. Yap. 2017. Mammalian Diaphanous 1 Mediates a Pathway for E-cadherin to Stabilize Epithelial Barriers through Junctional Contractility. *Cell Reports*. 18:2854–2867. <https://doi.org/10.1016/j.celrep.2017.02.078>
- Aoki, K., F. Maeda, T. Nagasako, Y. Mochizuki, S. Uchida, and J. Ikenouchi. 2016. A RhoA and Rnd3 cycle regulates actin reassembly during membrane blebbing. *Proc. Natl. Acad. Sci. USA*. 113:E1863–E1871. <https://doi.org/10.1073/pnas.1600968113>

- Balasubramanian, N., D.W. Scott, J.D. Castle, J.E. Casanova, and M.A. Schwartz. 2007. Arf6 and microtubules in adhesion-dependent trafficking of lipid rafts. *Nat. Cell Biol.* 9:1381–1391. <https://doi.org/10.1038/ncb1657>
- Barmeyer, C., J.D. Schulzke, and M. Fromm. 2015. Claudin-related intestinal diseases. *Semin. Cell Dev. Biol.* 42:30–38. <https://doi.org/10.1016/j.semcdb.2015.05.006>
- Chichili, G.R., and W. Rodgers. 2009. Cytoskeleton-membrane interactions in membrane raft structure. *Cell. Mol. Life Sci.* 66:2319–2328. <https://doi.org/10.1007/s00018-009-0022-6>
- del Pozo, M.A., N.B. Alderson, W.B. Kiosses, H.H. Chiang, R.G. Anderson, and M.A. Schwartz. 2004. Integrins regulate Rac targeting by internalization of membrane domains. *Science*. 303:839–842. <https://doi.org/10.1126/science.1092571>
- Diaz-Rohrer, B.B., K.R. Levental, K. Simons, and I. Levental. 2014. Membrane raft association is a determinant of plasma membrane localization. *Proc. Natl. Acad. Sci. USA*. 111:8500–8505. <https://doi.org/10.1073/pnas.1404582111>
- Francis, S.A., J.M. Kelly, J. McCormack, R.A. Rogers, J. Lai, E.E. Schneeberger, and R.D. Lynch. 1999. Rapid reduction of MDCK cell cholesterol by methyl-beta-cyclodextrin alters steady state transepithelial electrical resistance. *Eur. J. Cell Biol.* 78:473–484. [https://doi.org/10.1016/S0171-9335\(99\)80074-0](https://doi.org/10.1016/S0171-9335(99)80074-0)
- Furuse, M., H. Sasaki, K. Fujimoto, and S. Tsukita. 1998. A single gene product, claudin-1 or -2, reconstitutes tight junction strands and recruits occludin in fibroblasts. *J. Cell Biol.* 143:391–401. <https://doi.org/10.1083/jcb.143.2.391>
- Gumbiner, B., B. Stevenson, and A. Grimaldi. 1988. The role of the cell adhesion molecule uvomorulin in the formation and maintenance of the epithelial junctional complex. *J. Cell Biol.* 107:1575–1587. <https://doi.org/10.1083/jcb.107.4.1575>
- Hartsock, A., and W.J. Nelson. 2008. Adherens and tight junctions: structure, function and connections to the actin cytoskeleton. *Biochim. Biophys. Acta*. 1778:660–669. <https://doi.org/10.1016/j.bbame.2007.07.012>
- Hinck, L., I.S. Näthke, J. Papkoff, and W.J. Nelson. 1994. Dynamics of cadherin/catenin complex formation: novel protein interactions and pathways of complex assembly. *J. Cell Biol.* 125:1327–1340. <https://doi.org/10.1083/jcb.125.6.1327>
- Ikenouchi, J., and M. Umeda. 2010. FRMD4A regulates epithelial polarity by connecting Arf6 activation with the PAR complex. *Proc. Natl. Acad. Sci. USA*. 107:748–753. <https://doi.org/10.1073/pnas.0908423107>
- Ikenouchi, J., M. Suzuki, K. Umeda, K. Ikeda, R. Taguchi, T. Kobayashi, S.B. Sato, T. Kobayashi, D.B. Stolz, and M. Umeda. 2012. Lipid polarity is maintained in absence of tight junctions. *J. Biol. Chem.* 287:9525–9533. <https://doi.org/10.1074/jbc.M111.327064>
- Ikenouchi, J., M. Hirata, S. Yonemura, and M. Umeda. 2013. Sphingomyelin clustering is essential for the formation of microvilli. *J. Cell Sci.* 126:3585–3592. <https://doi.org/10.1242/jcs.122325>
- Lingaraju, A., T.M. Long, Y. Wang, J.R. Austin II, and J.R. Turner. 2015. Conceptual barriers to understanding physical barriers. *Semin. Cell Dev. Biol.* 42:13–21. <https://doi.org/10.1016/j.semcdb.2015.04.008>
- Maddugoda, M.P., M.S. Crampton, A.M. Shewan, and A.S. Yap. 2007. Myosin VI and vinculin cooperate during the morphogenesis of cadherin cell cell contacts in mammalian epithelial cells. *J. Cell Biol.* 178:529–540. <https://doi.org/10.1083/jcb.200612042>
- McNeill, H., T.A. Ryan, S.J. Smith, and W.J. Nelson. 1993. Spatial and temporal dissection of immediate and early events following cadherin-mediated epithelial cell adhesion. *J. Cell Biol.* 120:1217–1226. <https://doi.org/10.1083/jcb.120.5.1217>
- Meng, W., and M. Takeichi. 2009. Adherens junction: molecular architecture and regulation. *Cold Spring Harb. Perspect. Biol.* 1:a002899. <https://doi.org/10.1101/cshperspect.a002899>
- Mesmin, B., and B. Antonny. 2016. The counterflow transport of sterols and PI4P. *Biochim. Biophys. Acta*. 1861(8, 8 Pt B):940–951. <https://doi.org/10.1016/j.bbalip.2016.02.024>
- Nicolson, G.L. 2014. The Fluid-Mosaic Model of Membrane Structure: still relevant to understanding the structure, function and dynamics of biological membranes after more than 40 years. *Biochim. Biophys. Acta*. 1838:1451–1466. <https://doi.org/10.1016/j.bbame.2013.10.019>
- Norambuena, A., and M.A. Schwartz. 2011. Effects of integrin-mediated cell adhesion on plasma membrane lipid raft components and signaling. *Mol. Biol. Cell*. 22:3456–3464. <https://doi.org/10.1091/mbc.E11-04-0361>
- Nusrat, A., C.A. Parkos, P. Verkade, C.S. Foley, T.W. Liang, W. Innis-Whitehouse, K.K. Eastburn, and J.L. Madara. 2000. Tight junctions are membrane microdomains. *J. Cell Sci.* 113:1771–1781.
- Ogou, S.I., C. Yoshida-Noro, and M. Takeichi. 1983. Calcium-dependent cell-cell adhesion molecules common to hepatocytes and teratocarcinoma stem cells. *J. Cell Biol.* 97:944–948. <https://doi.org/10.1083/jcb.97.3.944>
- Pinto da Silva, P., and B. Kachar. 1982. On tight-junction structure. *Cell*. 28:441–450. [https://doi.org/10.1016/0092-8674\(82\)90198-2](https://doi.org/10.1016/0092-8674(82)90198-2)
- Sezgin, E., I. Levental, S. Mayor, and C. Eggeling. 2017. The mystery of membrane organization: composition, regulation and roles of lipid rafts. *Nat. Rev. Mol. Cell Biol.* 18:361–374. <https://doi.org/10.1038/nrm.2017.16>
- Shigetomi, K., and J. Ikenouchi. 2018. Regulation of the epithelial barrier by post-translational modifications of tight junction membrane proteins. *J. Biochem.* 163:265–272. <https://doi.org/10.1093/jb/mvx077>
- Shiomi, R., K. Shigetomi, T. Inai, M. Sakai, and J. Ikenouchi. 2015. CaMKII regulates the strength of the epithelial barrier. *Sci. Rep.* 5:13262. <https://doi.org/10.1038/srep13262>
- Stolz, D.B., G. Bannish, and B.S. Jacobson. 1992. The role of the cytoskeleton and intercellular junctions in the transcellular membrane protein polarity of bovine aortic endothelial cells in vitro. *J. Cell Sci.* 103:53–68.
- Takeichi, M. 2018. Multiple functions of α -catenin beyond cell adhesion regulation. *Curr. Opin. Cell Biol.* 54:24–29. <https://doi.org/10.1016/j.ceb.2018.02.014>
- Tokumasu, R., K. Yamaga, Y. Yamazaki, H. Murota, K. Suzuki, A. Tamura, K. Bando, Y. Furuta, I. Katayama, and S. Tsukita. 2016. Dose-dependent role of claudin-1 in vivo in orchestrating features of atopic dermatitis. *Proc. Natl. Acad. Sci. USA*. 113:E4061–E4068. <https://doi.org/10.1073/pnas.1525474113>
- Tsukita, S., M. Furuse, and M. Itoh. 2001. Multifunctional strands in tight junctions. *Nat. Rev. Mol. Cell Biol.* 2:285–293. <https://doi.org/10.1038/35067088>
- Watabe-Uchida, M., N. Uchida, Y. Imamura, A. Nagafuchi, K. Fujimoto, T. Uemura, S. Vermeulen, F. van Roy, E.D. Adamson, and M. Takeichi. 1998. α -Catenin-vinculin interaction functions to organize the apical junctional complex in epithelial cells. *J. Cell Biol.* 142:847–857. <https://doi.org/10.1083/jcb.142.3.847>
- Zihni, C., C. Mills, K. Matter, and M.S. Balda. 2016. Tight junctions: from simple barriers to multifunctional molecular gates. *Nat. Rev. Mol. Cell Biol.* 17:564–580. <https://doi.org/10.1038/nrm.2016.80>